High-performance optical wavelength-selective switches based on double ring resonators

Kambiz Abedi*

Department of Electrical Engineering, Faculty of Electrical and Computer Engineering, Shahid Beheshti University, Tehran 1983963113, Iran

(Received 26 January 2013)

In order to improve the performance of optical wavelength-selective switches based on double micro-ring resonators, an asymmetric intra-step-barrier coupled double strained quantum wells (AICD-SQWs) structure is utilized as the active light guiding medium. The AICD-SQW active layer has advantages, such as large change range in absorption coefficient, high extinction ratio, large Stark shift and very low insertion. For predicting the switching characteristics of double ring resonators structure, the absorption coefficient and real refractive index changes of the AICD-SQW active layer are calculated for different applied electric fields for TE input light polarization. Simulation results show that switching characteristics strongly depend on changes in absorption coefficient and real refractive index of active layer. In addition, isolations of 37.44 dB and 26.84 dB are realized between drop and through ports, when drop and through ports are ON and OFF, respectively, and vice versa.

Document code: A **Article ID:** 1673-1905(2013)03-0185-4

DOI 10.1007/s11801-013-3019-1

Optical wavelength-selective switches based on micro-ring resonators are attractive in modern dense wavelength division multiplexing (DWDM) and optical networks applications for the implementation of fundamental functions. The functions, such as channel add-drop, channel selection, demultiplexing and multichannel filtering, are formed due to narrow band filtering, high quality factor, compactness and functionality of micro-ring resonators in contrast to conventional integrated optics devices[1-5]. The structure of these switches is based on two coupled micro-ring resonators which are placed between two straight bus waveguides. The main task of the bus waveguides is not only to enable an efficient low loss fiber-chip coupling but also to facilitate a nearly "lossless" and monomodal propagation of the light within the chip. Most of wavelength-selective switch structures based on micro-ring resonators have a fixed response which are passive in the sense that once fabricated, no further adjustment or tunability is available to alter their spectral response. Recently, an active series coupled double micro-ring resonators structure using quantum wells (QWs) based on $In_yGa_{1-y}As_{1-x}P_x$ materials as the active region has been proposed[4]. In this structure, by applying a voltage, absorption of the QW at resonant wavelength changes and the resonant condition of the micro-ring, and switching of the resonant wavelength from the drop port to transmit port are modified. On the other hand, in the previous works of the author[6-16], we have introduced asymmetric intra-step-barrier coupled double strained quantum wells (AICD-SQWs) structure which has been demonstrated to suppress the red shift of the quantum confined Stark effect (QCSE) to a higher electric field and to reduce the oscillator intensity at zero field[6,7]. Compared with coupled double strained quantum wells, the AICD-SQWs structure can deeply separate electron and heavy hole wave functions at zero electric field, thereby decreasing the insertion loss. Due to the increased operation electric field and the decreased spatial overlap integral between the electron and the hole envelope wave functions, the asymmetric coupled quantum wells double micro-ring resonators based optical wavelength-selective switches have higher saturation optical power, larger Stark shift, larger change in absorption, higher extinction ratio and lower insertion loss than the conventional QW. This paper intends to improve the performance of the optical wavelength-selective switches based on double ring resonators with AICD-SQWs structure as the active light guiding medium.

A schematic diagram of optical wavelength-selective switch based on two micro-ring resonators with electro-absorption AICD-SQW active layer[4,6] is shown in Fig.1. In this configuration, the dropped wavelength and input wavelength are propagating along the same direction. But through separate channels, making the interconnection of many such devices practical, and among a series of wavelengths launched at the input, only the resonant wavelength appears at the drop port, while non-resonant wavelengths bypass the rings and appear at the transmit port. Active region consists of an intrinsic eight-period AICD-SQW,

* E-mail: k_abedi@sbu.ac.ir

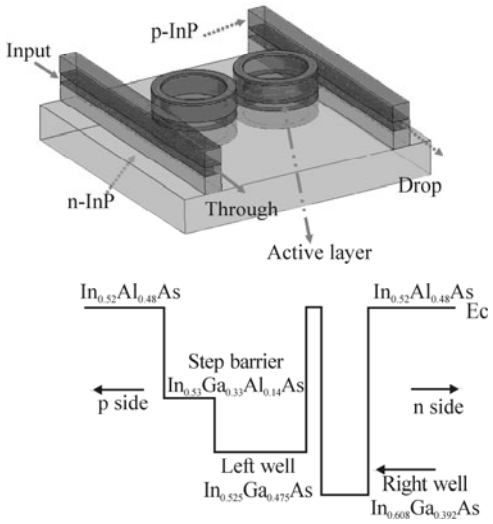

Fig.1 Wavelength-selective switch based on two micro-ring resonators with electro-absorption AlCD-SQWs active layer

separated with 10 nm-thick $In_{0.52}Al_{0.48}As$ barriers which are lattice matched to InP. Each period of the proposed AlCD-SQW consists of a 4 nm-thick $In_{0.53}Ga_{0.33}Al_{0.14}As$ intra-step-barrier, a 1.5 nm-thick $In_{0.52}Al_{0.48}As$ as the narrow barrier, a 6.8 nm-thick $In_{0.525}Ga_{0.475}As$ (0.05% tensile strain) for the left well and a 3.5 nm-thick $In_{0.608}Ga_{0.392}As$ (0.52% compressive strain) for the right well[6-8]. The ratios of transmitted and dropped power to input power are given as[4]

$$\left|\frac{E_{\mathrm{T}}}{E_{\mathrm{I}}}\right|=\left|\frac{\tau_a \mathrm{e}^{\left(\frac{2\mathrm{j}\omega n_{\mathrm{r}}L}{c}-\alpha L\right)}-\tau_b\left(1+\tau_a^2\right)\mathrm{e}^{\left(\frac{\mathrm{j}\omega n_{\mathrm{r}}L}{c}-\frac{\alpha L}{2}\right)}+\tau_a}{1-2\tau_a\tau_b\mathrm{e}^{\left(\frac{\mathrm{j}\omega n_{\mathrm{r}}L}{c}-\frac{\alpha L}{2}\right)}+\tau_a^2\mathrm{e}^{\left(\frac{2\mathrm{j}\omega n_{\mathrm{r}}L}{c}-\alpha L\right)}}\right|^2, \quad (1)$$

$$\left|\frac{E_{\mathrm{D}}}{E_{\mathrm{I}}}\right|=\left|\frac{\mathrm{j}\kappa_a^2\kappa_b\mathrm{e}^{\left(\frac{\mathrm{j}\omega n_{\mathrm{r}}L}{c}-\frac{\alpha L}{2}\right)}}{1-2\tau_a\tau_b\mathrm{e}^{\left(\frac{\mathrm{j}\omega n_{\mathrm{r}}L}{c}-\frac{\alpha L}{2}\right)}+\tau_a^2\mathrm{e}^{\left(\frac{2\mathrm{j}\omega n_{\mathrm{r}}L}{c}-\alpha L\right)}}\right|, \quad (2)$$

where τ_a and κ_a are the transmission and coupling coefficient at the coupling regions where the ring is in close proximity to the waveguide, while τ_b and κ_b are the transmission and coupling coefficient at the coupling regions where the rings are coupled between themselves, respectively. $L = 2\pi R$ is the circumference of the ring, and R is the radius of the ring. $\omega = 2\pi c/\lambda$ represents the angular frequency of the circulating light. Furthermore, n_{r} is the real refractive index, and α is the absorption coefficient of the undoped AlCD-SQW active layer of the rings[6,7], as dropped and transmitted power is strongly dependent on them. Therefore, the absorption spectrum and refractive index of the undoped AlCD-SQW active layer of the rings are required to characterize the ratios of transmitted and dropped power to input power. The electro-absorption spectrum $\alpha(h\nu)$ is related to the imaginary part of the dielectric constant $\varepsilon_{\mathrm{i}}(h\nu)$, which is given as[6]:

$$\alpha(h\nu)=\frac{2\pi}{\lambda_0 n_{\mathrm{r}}}\varepsilon_{\mathrm{i}}(h\nu)=\frac{\omega}{cn_{\mathrm{r}}}\varepsilon_{\mathrm{i}}(h\nu), \quad (3)$$

where λ_0, c and n_{r} are the free-space wavelength of incident light, the speed of light in vacuum and the real refractive index, respectively. $\alpha(h\nu)$ can be defined as:

$$\alpha(h\nu)=\alpha(h\nu)^{\mathrm{band}}+\alpha(h\nu)^{\mathrm{exciton}}. \quad (4)$$

The first term is due to the band-to-band transitions, and the second term is due to the excitonic transitions. The electro-absorption coefficient of the band-to-band transitions between nth subband electrons and mth subband holes is written as[6]:

$$\alpha(h\nu)^{\mathrm{band}}=\frac{e^2}{\varepsilon_0 m_0^2 cn_{\mathrm{r}}\omega L_z}\cdot\frac{\mu}{\hbar^2}\int M_{nm}^2(E)\cdot L(h\nu-E-E_{\mathrm{g}}-E_n^e-E_m^h)\mathrm{d}E, \quad (5)$$

where ε_0 is the dielectric constant, m_0 is the free-electron mass, n_{r} is the refractive index, L_z is the effective thickness of the AlCD-SQW, E_{g} is the energy gap, μ is the reduced mass for the motion in the xy plane, and $L(y)$ is the line shape function for each transition. The electro-absorption coefficient of an exciton transition is written as:

$$\alpha(h\nu)^{\mathrm{exciton}}=\frac{\pi e^2\hbar}{n_{\mathrm{r}}\varepsilon_0 m_0 cL_z}\sum_X f_X L(h\nu-E_X), \quad (6)$$

where the exciton oscillator strength for this state is defined as[6]:

$$f_X=\frac{2}{m_0 E_X}\left|\int\frac{\mathrm{d}^2k}{(2\pi)^2}\phi_{nm}^X(k)M_{nm}(k)\right|^2, \quad (7)$$

where $\phi_{nm}^X(k)$ is the exciton envelop wave function in momentum space, and the exciton binding energy is given by :

$$E_{\mathrm{B}}=E_X-E_n^e-E_m^h-E_{\mathrm{g}}. \quad (8)$$

On the other hand, the change of real refractive index can be obtained from the change of absorption coefficient by the Kramers-Kronig relation[10]:

$$\Delta n_{\mathrm{r}}(\lambda_0,F)=\frac{\lambda_0^2}{2\pi^2}\mathrm{P.V.}\int_0^\infty\frac{\Delta\alpha(\lambda,F)}{\lambda_0^2-\lambda^2}\mathrm{d}\lambda=\frac{\lambda_0^2}{2\pi^2}\left[\lim_{\varepsilon\to0}\int_0^{\lambda_0-\varepsilon}\frac{\Delta\alpha(\lambda,F)}{\lambda_0^2-\lambda^2}\mathrm{d}\lambda+\lim_{\varepsilon\to0}\int_{\lambda_0+\varepsilon}^\infty\frac{\Delta\alpha(\lambda,F)}{\lambda_0^2-\lambda^2}\mathrm{d}\lambda\right], \quad (9)$$

where P.V. stands for the Cauchy principal value, and F is the electric field. The details of the calculation approach of absorption coefficient and refractive index are given by Abedi et al[6,7]. The calculated electro-absorption spectra of the AlCD-SQW structure for TE mode with different values of applied electric field are shown in

Fig.2. The two peaks in the electro-absorption spectra depict electron-heavy hole and electron-light hole transitions, respectively. Electrons and holes are confined thoroughly in the tensile wide well and compressive narrow well at F=0 kV/cm, respectively. Furthermore, the height of the exciton peak in the AICD-SQW structure increases quickly when the applied electric field is smaller than 36.70 kV/cm (blue shift), then gradually decreases with further increasing of applied electric field (red shift)[6].

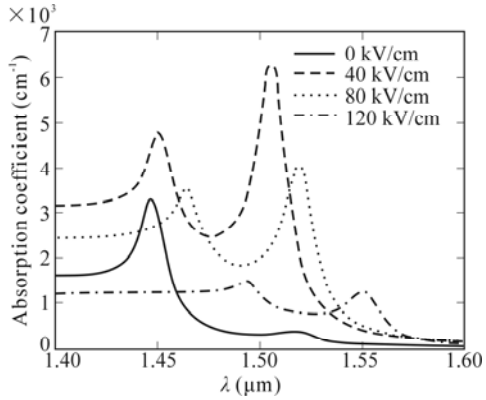

Fig.2 Calculated electro-absorption spectra for TE mode in AICD-SQW structure

The change of absorption coefficient between the ON and OFF states ($\Delta\alpha$) is obtained from the calculated absorption curves for different applied electric fields by subtracting the values of different electrical fields from that of the lowest non-zero electrical field. Fig.3 shows the change in absorption coefficient ($\Delta\alpha$) of the AICD-SQW for applied electric fields of 40 kV/cm, 80 kV/cm and 120 kV/cm.

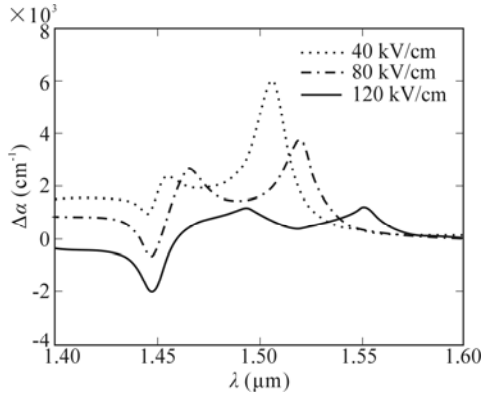

Fig.3 Change in absorption coefficient for TE mode in AICD-SQW structure

Any change of absorption due to applied F leads to a change of real refractive index, and this index change is calculated by using Kramers-Kronig relations. Fig.4 shows the real refractive index change as a function of wavelength with varying applied field for TE mode in AICD-SQW structure.

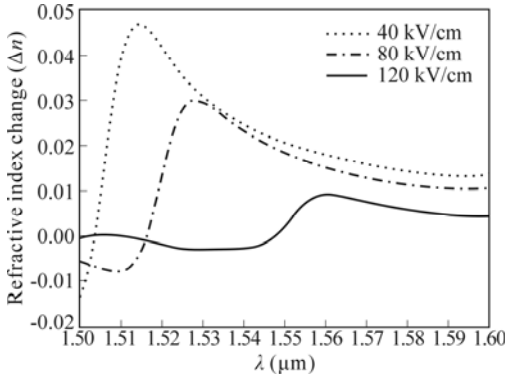

Fig.4 Change of real refractive index versus wavelength with various applied fields for TE mode in AICD-SQW structure

For double micro-ring resonators structure with a fixed radius, there can be several wavelengths which can resonate, but the operating resonant wavelength is fixed. In this case, we select R as 1.2248 μm, and hence the resonant wavelength is 1.55 μm which is the wavelength of our interest. The effective index of the AICD-SQW is considered as 3.6255[6,9]. The resonant wavelength of 1.55 μm couples to the ring, and appears at the drop port without applied F. In this state, the output power at the drop port is slightly less than the input power due to insertion loss. When F=120 kV/cm, we find that absorption in the ring is increased to a high value of 1.414×10^3 cm^{-1} at wavelength of 1.55 μm, which results in the wavelength of 1.55 μm appearing at through port. Fig.5 shows the switching characteristics of double micro-ring

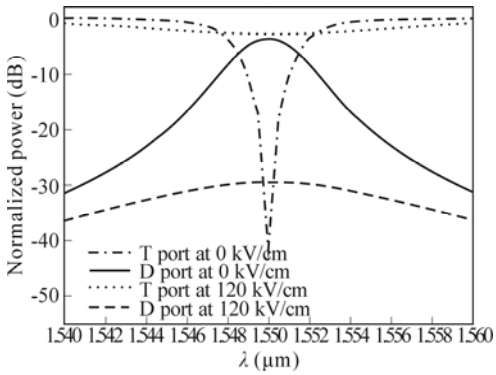

Fig.5 Switching characteristics at the drop and through ports for double micro-ring resonators structure

resonators structure when the applied field varies from 0 kV/cm to 120 kV/cm. In this case, the change of real refractive index Δn_r is calculated as 2.129×10^{-3} which makes the resonant wavelength of double micro-ring resonators structure red shift. In the calculations, κ_a and κ_b are considered 0.4 and $0.5\times\kappa_a^2$, respectively. From Fig.5, we find that for the resonant wavelength of 1.55 μm, at F=0 kV/cm which corresponds to the absorption coefficient of 92.58 cm^{-1}, the optical intensities at through port and drop port are −41.19 dB and −3.75 dB,

respectively, which corresponds to an isolation of 37.44 dB between drop and through ports, and thus, drop port is ON and through port is OFF.

For F = 60 kV/cm which corresponds to absorption coefficient of 1.414×10^3 cm^{-1}, optical intensities at through port and drop port are −2.78 dB and −29.62 dB, respectively, which corresponds to an isolation of 26.84 dB between drop and through ports, and thus, through port is now ON, and drop port is OFF. Thus absorption switches the resonant wavelength of 1.55 μm from drop to through port. The use of electro-absorption as switching mechanism in double micro-ring resonators structure means that the device speed is much higher compared with switches which use carrier injection or thermo-optic effects, due to the fast response of electro-absorption effect. Compared with a Mach-Zehnder interferometer switch or directional coupler switch, the device size of the double ring resonators switch will be much smaller[4].

References

[1] B. E. Little, S. T. Chu, H. A. Hauss, J. Foresi and J. P. Laine, IEEE J. Lightw. Technol. **15**, 998 (1997).

[2] T. Barwicz, M. A. Popovic, P. T. Rakich, M. R. Watts, H. A. Haus, E. P. Ippen and H. I. Smith, Opt. Express **12**, 1437 (2004).

[3] K. Takahashi, Y. Kanamori, Y. Kokubun and K. Hane, Opt. Express **16**, 14421 (2008).

[4] S. Ravindran, K. Alameh and Y. T. Lee, Opt. Quant. Electron. **41**, 635 (2009).

[5] R. Grover, T. A. Ibrahim, S. Kanakaraju, L. Lucas, L. C. Calhoun and P. H. Ho, IEEE Photon. Technol. Lett. **16**, 467 (2004).

[6] K. Abedi, V. Ahmadi, E. Darabi, M. K. Moravvej-Farshi and M. H. Sheikhi., Solid State Electron. **53**, 312 (2008).

[7] K. Abedi, Eur. Phys. J. Appl. Phys. **56**, 10403 (2011).

[8] K. Abedi, V. Ahmadi and M. K. Moravvej-Farshi, Opt. Quant. Electron. **41**, 719 (2009).

[9] K. Abedi, Opt. Quant. Electron. **44**, 55 (2012).

[10] K. Abedi, J. Semicond. **33**, 064001 (2012).

[11] K. Abedi, Optoelectron. Lett. **8**, 176 (2012).

[12] K. Abedi, Int. J. Eng. Sci. Technol. **3**, 6684 (2011).

[13] K. Abedi, Int. J. Adv. Eng. Technol. **1**, 388 (2011).

[14] K. Abedi, Canad. J. Electric. Electron. Eng. **2**, 209 (2011).

[15] K. Abedi and H. Afrouz, Acta Physica Polonica A **123**, 415 (2013).

[16] K. Abedi, International Review of Modelling and Simulations (IREMOS) **4**, 1982 (2011).